Development 128, 2989-3000 (2001)
Printed in Great Britain © The Company of Biologists Limited 2001
DEV2739

Forebrain and midbrain development requires epiblast-restricted *Otx2* translational control mediated by its 3′ UTR

Pietro Pilo Boyl[1,*], Massimo Signore[1,2,*], Dario Acampora[1,2,*], Juan Pedro Martinez-Barbera[1], Cristina Ilengo[3], Alessandro Annino[2], Giorgio Corte[3,4] and Antonio Simeone[1,2,‡]

[1]MRC Centre for Developmental Neurobiology, King's College London, Guy's Campus, New Hunt's House, London SE1 1UL, UK
[2]International Institute of Genetics and Biophysics, CNR, Via G. Marconi 12, 80125, Naples, Italy
[3]IST-National Institute for Cancer Research, Università di Genova, Largo Benzi, 16132 Genova, Italy
[4]Dipartimento di Oncologia Clinica e Sperimentale, Università di Genova, Largo Benzi, 16132 Genova, Italy
*These authors contributed equally to this work
‡Author for correspondence (e-mail: antonio.simeone@kcl.ac.uk)

Accepted 8 May 2001

SUMMARY

Otx genes play an important role in brain development. Previous mouse models suggested that the untranslated regions (UTRs) of *Otx2* mRNA may contain regulatory element(s) required for its post-transcriptional control in epiblast and neuroectoderm. In order to study this, we have perturbed the 3′ UTR of *Otx2* by inserting a small fragment of DNA from the λ phage. *Otx2*$^{\lambda}$ mutants exhibited proper gastrulation and normal patterning of the early anterior neural plate, but from 8.5 days post coitum they developed severe forebrain and midbrain abnormalities. OTX2 protein levels in *Otx2*$^{\lambda}$ mutants were heavily reduced in the epiblast, axial mesendoderm and anterior neuroectoderm but not in the visceral endoderm. At the molecular level, we found out that the ability of the *Otx2*$^{\lambda}$ mRNA to form efficient polyribosome complexes was impaired. Sequence analysis of the *Otx2*-3′ UTR revealed a 140 bp long element that is present only in vertebrate *Otx2* genes and conserved in identity by over 80%. Our data provide experimental evidence that murine brain development requires accurate translational control of *Otx2* mRNA in epiblast and neuronal progenitor cells. This leads us to hypothesise that this control might have important evolutionary implications.

Key words: *Otx2*, Translational control, 3′ UTR, Visceral endoderm, Epiblast, Brain evolution, Mouse

INTRODUCTION

Understanding how genetic functions are translated into phenotype represents a basic issue when studying morphogenetic mechanisms of development (Holland, 1999). Indeed, molecular events such as gene duplication, modification of regulatory control and establishment of new functions may result in an increased complexity of the body plan and in the generation of new cell types. In particular, understanding whether modification in the regulatory control of highly conserved genes may influence morphogenetic processes that underlie vertebrate brain development represents an important achievement. A remarkable amount of data have been collected in the last few years on the role of gene candidates for controlling developmental programmes that underlie brain morphogenesis (Acampora and Simeone, 1999; Beddington and Robertson, 1999; Stern, 2001; Wurst and Bally-Cuif, 2001). Most of these genes are the vertebrate homologues of *Drosophila* genes that code for signal molecules or transcription factors (Crossley et al., 1996; De Robertis and Sasai, 1996; Tam and Behringer, 1997; Rubenstein et al., 1998; Reichert and Simeone, 1999). Among these, the *orthodenticle* group includes the *Drosophila orthodenticle* (*otd*) and the vertebrate *Otx1* and *Otx2* genes, both of which contain a *bicoid*-like homeodomain (Simeone et al., 1992; Simeone et al., 1993, Simeone, 1998).

Otx1 and *Otx2* animal models (*Otx1* knockout; *Otx2* knockout; *Otx1/Otx2* double mutant) have indicated that these two genes play a key role in brain and sense organ development. Indeed, *Otx1* is required for corticogenesis and the differentiation of visual and acoustic sense organ structures (Acampora et al., 1996), while *Otx2* for early specification of the neuroectoderm fated to become the fore-mid and rostral hindbrain (Acampora et al., 1995; Matsuo et al., 1995; Ang et al., 1996). Both Otx genes are required for brain regionalisation and patterning (Acampora et al., 1997; Suda et al., 1997).

Further studies on chimaeric embryos and mouse models have allowed the uncoupling of *Otx2* requirements and assigned them to two distinct phases and cell types: early induction of anterior neural patterning, under visceral endoderm (VE) control, and its subsequent maintenance, mediated by epiblast-derived cells such as axial mesendoderm (ame) and anterior neuroectoderm (ane) (Acampora et al., 1998b; Rhinn et al., 1998; Acampora and Simeone, 1999; Beddington and Robertson, 1999).

In particular, the analysis of embryos in which *Otx2* is

replaced with a human *Otx1* cDNA has also revealed that while the human *OTX1* mRNA is transcribed in both the VE and epiblast, the human OTX1 protein is synthesised only in the VE. This VE-restricted translation was sufficient to recover *Otx2* requirements for the specification of anterior neural patterning and proper organisation of the primitive streak, but it failed to maintain anterior patterning (Acampora et al., 1998b).

This unexpected phenomenon has suggested the possibility that a differential post-transcriptional control may exist between VE and epiblast, and that the *Otx2* replaced region, including 200 bp of the 5′ untranslated region (UTR), the entire coding region, introns and the 3′ UTR, may contain regulatory elements required for epiblast-restricted translation of *Otx2* mRNA. To address this issue, we have generated a mouse model that carries a 300 bp long insertion of exogenous DNA from the λ phage into the 3′ UTR of *Otx2* with the aim of perturbing its post-transcriptional control.

We report that 65% of the homozygous $Otx2^{\lambda}/Otx2^{\lambda}$ embryos exhibited head abnormalities with exencephaly and microcephaly, while 100% of embryos carrying one copy of the mutated allele in an *Otx2* null background ($Otx2^{\lambda}/-$) showed a severe reduction of the rostral brain. A detailed analysis has revealed that, when compared with the wild type, the $Otx2^{\lambda}$ mRNA was properly distributed in the embryo, its level was slightly reduced, while the amount of protein was drastically diminished in epiblast, ame and ane, owing to an impairment of its ability to form efficient polyribosome complexes. Interestingly, alignment of *Otx2*-3′ UTR sequences from several species has revealed a 140 bp long element that is conserved only in vertebrate *Otx2* genes.

These findings provide experimental evidence that, in mouse, proper brain development requires accurate translational control of *Otx2* in epiblast cells and their derivatives in order to establish *Otx2*-dependent maintenance properties of forebrain and midbrain territory. Furthermore, we also hypothesise that the establishment of this type of translational control seems to correlate with the transition to a more complicated vertebrate brain, that of gnathostomes (jawed vertebrates).

MATERIALS AND METHODS

Targeting vector, ES cell transfection and selection of targeted clones

In order to generate the targeting vector, two adjacent genomic regions in the *Otx2* locus, a 4.8 kb long *Apa*I fragment, and a 0.9 kb long *Apa*I/*Kpn*I fragment were cloned flanking a neomycin cassette into the pGN plasmid (Acampora et al., 1995; Fig. 1A).

The λ tag, a 297 bp long fragment corresponding to position 5218-5514 of the λ phage sequence was introduced by PCR mutagenesis in the 3′ UTR of *Otx2* 51 bp downstream of the stop codon and then in the long arm of the targeting vector. HM-1 ES homologous recombinant clones were identified by a PCR reaction using the following oligonucleotides: sense primer, 5′-TGCTGTGTTCCAGA-AGTGTT-3′; antisense primer, 5′-GATTTGCAGGCACGGC-TAGGATGA-3′ (arrows in Fig. 1A) and confirmed by hybridising *Eco*RI-digested genomic DNA with probes (b) and (e) in Fig. 1A,B.

Mouse production and genotyping

Two independent positive clones were injected into C57BL/6 blastocysts and the resulting chimaeric males back-crossed to B6/D2 F1 females. Genotyping was performed by PCR using two primers specific for the wild-type allele (open arrowheads in Fig. 1A; sense primer, AGATCATCCTGGACTTGGAG; antisense primer, CCCTT-TCCTTGCTAAAGTTTCC) and two primers specific for the λ sequence (black arrowheads in Fig. 1A; sense primer, AACTGCAGT-GTACAGCGGTCA; antisense primer, GGATCCCCATAATG-CGGCT). These primers amplify two DNA fragments 234 and 300 bp long, respectively (Fig. 1C).

RNAse protection assay

RNAse protection was performed as previously described (Simeone et al., 1993). In order to analyse $Otx2^{\lambda}$ and wild-type *Otx2* mRNA in the same assay, we used a 200 bp long PCR fragment that contained 15 bp of the λ sequence and 185 bp further upstream in the *Otx2* sequence (probe c in Fig. 1A). Phosphorimager scanning was performed to quantify RNA levels. For the in vitro synthesised $Otx2^{\lambda}$ RNA (see Fig. 5B), we used as template a 1.5 kb clone containing the λ tag and the entire *Otx2* coding sequence.

Western blot analysis

For each genotype total extracts were prepared from three independent pools of five or seven embryos at 7.5 d.p.c. These extracts (10 μg) were processed for standard western blot assay and probed with αOTX2 antiserum (1:5000; Mallamaci et al., 1996; Acampora et al., 1998b). Films were processed for densitometric scanning.

Polysome gradients and RNA purification

Sucrose gradients were performed essentially as described (Loreni and Amaldi, 1992). Gradients were collected in nine fractions of 1 ml each. An ultarviolet (254 nm) absorbance profile of the gradient was produced by ribosomal RNA while flowing through a spectrophotometer, in order to assign to each fraction the number of ribosomes bound to mRNA. Gels were processed for phosphorimager scanning and polysome gradient profiles were determined by calculating the values of each fraction as percentage of the total hybridisation signal.

Nuclear and cytoplasmic RNAs were isolated with a similar procedure from 10.5 d.p.c. heads. Nuclei were lysed in 400 μl of 2% SDS and 1 μg/ml proteinase K.

Immunohistochemistry

For immunohistochemistry, embryos were processed as previously reported (Acampora et al., 1998b). $Otx2^{\lambda}/Otx2^{\lambda}$ were generated by intercrossing surviving $Otx2^{\lambda}/Otx2^{\lambda}$ mice. A total of 20 $Otx2^{+/-}$, 20 $Otx2^{\lambda}/Otx2^{\lambda}$ and 14 $Otx2^{\lambda}/-$ embryos was analysed.

In situ hybridisation and probes

In situ hybridisation experiments on sections and whole embryos were performed as previously described (Hogan et al., 1994; Simeone, 1999).

Probes for *Wnt1*, *BF1* (*Foxg1* – Mouse Genome Informatics), *Fgf8*, *Six3*, *Gbx2*, *Cer-l* (*Cer1* – Mouse Genome Informatics) and *Lim1* (*Lhx1* – Mouse Genome Informatics) were the same previously described (Acampora et al., 1997; Acampora et al.,, 1998b). The *Chd* probe spanned nucleotide 145 to 2016 of the full-length mouse cDNA. The λ probe (probe d in Fig. 1A) was a PCR fragment corresponding to the λ DNA insertion. The *Otx2* probe employed in in situ hybridisation experiments on gastrulating wild-type embryos was probe (a) in Fig. 1A. The *Otx2* probe for whole-mount in situ hybridisation was a murine fragment containing the entire coding sequence.

Sequence analysis

Bestfit analysis between zebrafish (Li et al., 1994; Accession Number U14592) and mouse *Otx2*-3′ UTRs highlighted the conserved element of 140 bp. FastA (GCG program package, EMBL, Heidelberg) search performed on the GenEMBL and GenBank EST databases with the

140 bp element retrieved the same region from human (Accession Number AC023079, chromosome 14) and rat *Otx2* genes, only. No significant homology was detected with any other sequence.

By using Stringsearch program from the GCG package, the Otx2 cDNA sequences from sea urchin (Sakamoto et al., 1997; Accession Number AB011526), *Ascidia* (Wada et al., 1996; Accession Number D84062), *Amphioxus* (Williams and Holland, 1998; Accession Number AF043740), lamprey (Ueki et al., 1998; Accession Number AB012299) and *Xenopus* (Blitz and Cho, 1995; Accession Number U19813) were identified. The *Xenopus Otx2*-3′ UTR sequence was incomplete and was extended through a series of homology searches (ESTs AI031472 and AI031473) and cDNA sequencing. *Drosophila otd* mRNA has been reported by Filkenstein et al. (Filkenstein et al., 1990), and in the genome clone accession number AE003444. Chicken *Otx2* mRNA was cloned and sequenced.

The *Otx2*-3′ UTR regions from the different species were analysed with the Bestfit program from the GCG package and the BioEdit program.

RESULTS

Generation of the *Otx2*$^{\lambda}$ mouse mutant

A 300 bp long sequence, randomly chosen and amplified from the λ phage DNA was inserted 51 bp downstream of the *Otx2* stop codon. A 4.8 kb *Apa*I fragment, spanning a region containing *Otx2* second and third exons, and a 0.9 kb *Apa*I/*Kpn*I fragment adjacent to the former, were inserted with the same orientation in the pGN targeting plasmid (Acampora et al., 1995), where these two fragments flank a neomycin cassette (see Materials and Methods). The targeting vector was electroporated into HM-1 ES cells. Homologous recombination events resulted into an *Otx2* locus without any other alterations but for the λ tag insertion and the presence of the plasmid sequence 1 kb downstream of the *Otx2* nuclear polyadenylation sequence (Fig. 1A). Two independent homologous recombinant clones carrying the λ tag (Fig. 1B and Materials and Methods) were selected and injected into C57BL/6 blastocysts to generate chimaeric mice for germline transmission of the mutated allele. Heterozygotes *Otx2*$^{\lambda}$/*Otx2* identified by allele-specific PCR reactions (Fig. 1C) were healthy and fertile. Correct expression of the *Otx2*$^{\lambda}$ mutated allele was monitored in *Otx2*$^{\lambda}$/*Otx2* embryos at 6.5, 7.5, 8.5 and 10.5 days post coitum (d.p.c.; Fig. 1D and see below) by using the λ-specific probe (probe d in Fig. 1A).

Table 1. Phenotypic analysis of brain abnormalities in 10.5 d.p.c. *Otx2*$^{\lambda}$ embryos

Genotype	Phenotype			Embryos scored
	Normal	Moderate	Severe	
Otx2$^{\lambda}$/*Otx2*$^{\lambda}$	19 (35%)	29 (54%)	6 (11%)	54
Otx2$^{\lambda}$/–	0	5 (10%)	41 (90%)	46

Head abnormalities in *Otx2*$^{\lambda}$ mutants

Morphology of *Otx2*$^{\lambda}$ mutant embryos was analysed at 8, 10.5 and 16 d.p.c. At 8 d.p.c. no obvious abnormalities were detected in *Otx2*$^{\lambda}$/*Otx2*$^{\lambda}$ and *Otx2*$^{\lambda}$/– embryos (data not shown). At 10.5 d.p.c. 65% of the *Otx2*$^{\lambda}$/*Otx2*$^{\lambda}$ embryos exhibited brain abnormalities (Table 1). Phenotypic sorting showed that 54% of them (Table 1) presented moderate brain defects with exencephaly, lack of closure of neural tube (Fig. 2B) or microcephaly with midbrain and forebrain reduction (Fig. 2C), and 11% of them displayed severe brain defects (Table 1) with heavy reduction of forebrain and midbrain (data not shown). No obvious abnormalities were detected on the residual *Otx2*$^{\lambda}$/*Otx2*$^{\lambda}$ embryos and 10% of *Otx2*$^{\lambda}$/*Otx2*$^{\lambda}$ mutants were viable and fertile, even though they exhibited reduction in fertility and, occasionally, abnormal motor activity.

Despite the partially penetrant phenotype observed in *Otx2*$^{\lambda}$/*Otx2*$^{\lambda}$ mutants, 90% of 10.5 d.p.c. embryos carrying a

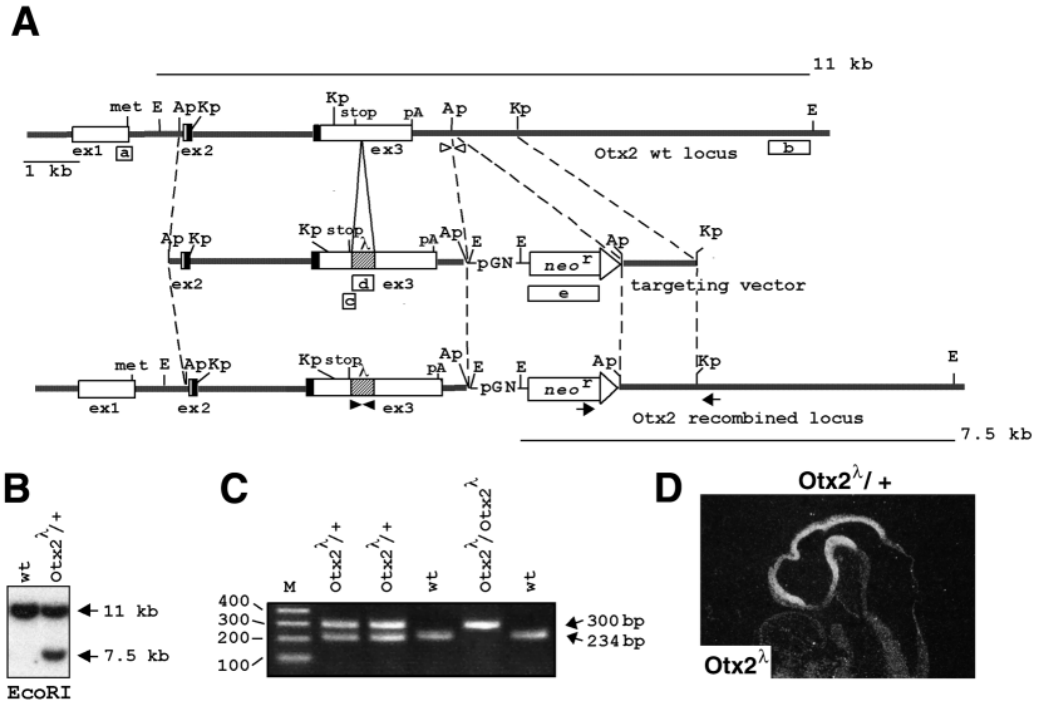

Fig. 1. Targeted mutagenesis of the 3′ UTR of the *Otx2* gene. (A) The targeting vector is shown in third line; fourth line illustrates recombined locus; first and last lines show *Eco*RI fragments (11 and 7.5 kb) detected by Southern blot using probes (a-e, white boxes) external to the targeting vector or within neomycin gene. Kp, *Kpn*I; Ap *Apa*I; E, *Eco*RI; met, methionine; stop, stop codon; pA: polyadenylation signal. (B) Southern blot analysis of one targeted cell line (*Otx2*$^{\lambda}$*/+*) and wild-type HM-1 ES cells hybridised with probe b in A. (C) PCR genotyping of a litter from two heterozygotes using the primers indicated as filled and open arrowheads in A. (D) In situ hybridisation of an *Otx2*$^{\lambda}$/*Otx2* embryo at 10 d.p.c. with the *Otx2*$^{\lambda}$-specific probe (probe d in A).

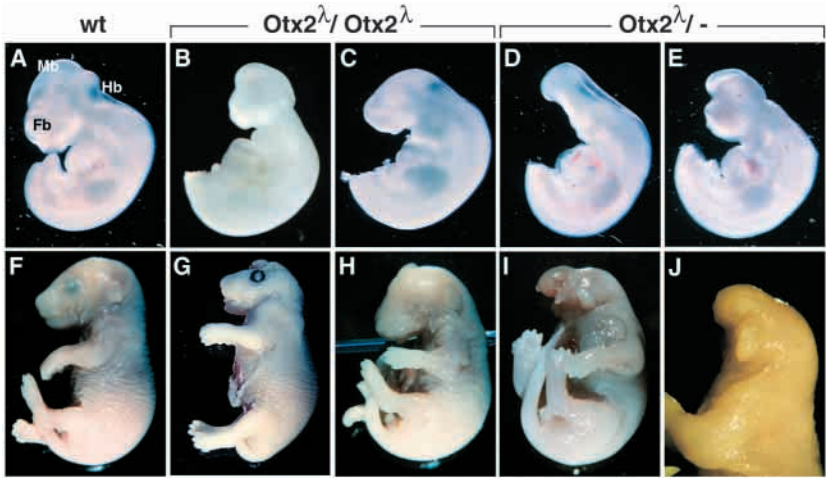

Fig. 2. Morphology of *Otx2*$^{\lambda}$/*Otx2*$^{\lambda}$ and *Otx2*$^{\lambda}$/– embryos. (A-J) When compared with wild-type (A,F), *Otx2*$^{\lambda}$/*Otx2*$^{\lambda}$ embryos exhibited brain abnormalities, the majority of which were exencephaly, lack of closure of neural tube (B,G) or reduction of forebrain-midbrain (C,H); 90% of *Otx2*$^{\lambda}$/– embryos revealed a severe reduction of anterior CNS with an almost headless phenotype (D,I,J) and 10% of them a phenotype (E) similar to that of *Otx2*$^{\lambda}$/*Otx2*$^{\lambda}$ mutants. Fb, forebrain; Hb, hindbrain; Mb, midbrain.

single *Otx2*$^{\lambda}$ allele in an *Otx2* null background (*Otx2*$^{\lambda}$/–) exhibited a severe reduction of rostral central nervous system (CNS; Fig. 2D and Table 1) and the residual 10% showed a moderate phenotype (Fig. 2E and Table 1). At 16 d.p.c., *Otx2*$^{\lambda}$/*Otx2*$^{\lambda}$ embryos showed different grades of brain abnormalities (Fig. 2G,H) frequently with anencephalic features, and *Otx2*$^{\lambda}$/– embryos displayed an almost headless phenotype that was characterised by the presence of a morphologically undefined neural structure (Fig. 2I,J). More than 90% of the *Otx2*$^{+/-}$ mice kept in the same genetic background (C57BL6/DBA2) were healthy and fertile.

Furthermore, in all the *Otx2*$^{\lambda}$/– embryos heavy abnormalities in the maxillary process and mandibular arch, as well as in their derivatives, were observed (Fig. 2D,E,I,J).

OTX2$^{\lambda}$ protein was specifically reduced in epiblast and its derivatives

The morphology of *Otx2*$^{\lambda}$/– embryos has led us to suspect that during gastrulation *Otx2*$^{\lambda}$ mRNA and/or protein may be affected. Hence, *Otx2* and *Otx2*$^{\lambda}$ transcripts and proteins were analysed at early streak (6.5 d.p.c.) and late streak/early headfold stages (7.75 d.p.c.) in wild-type, *Otx2*$^{+/-}$, *Otx2*$^{\lambda}$/*Otx2*$^{\lambda}$ and *Otx2*$^{\lambda}$/– embryos (Fig. 3).

While *Otx2*$^{+/-}$ and *Otx2*$^{\lambda}$/– embryos were genotyped by in situ hybridisation of adjacent sections with allele specific probes (Acampora et al., 1995; see also Materials and Methods), *Otx2*$^{\lambda}$/*Otx2*$^{\lambda}$ were generated by intercrossing viable *Otx2*$^{\lambda}$/*Otx2*$^{\lambda}$ mice. In Fig. 3 only the expression pattern of *Otx2* (Fig. 3A,B,E,F) and *Otx2*$^{\lambda}$ (Fig. 3C,D,G,H) was shown.

When compared with wild-type and *Otx2*$^{+/-}$ embryos,

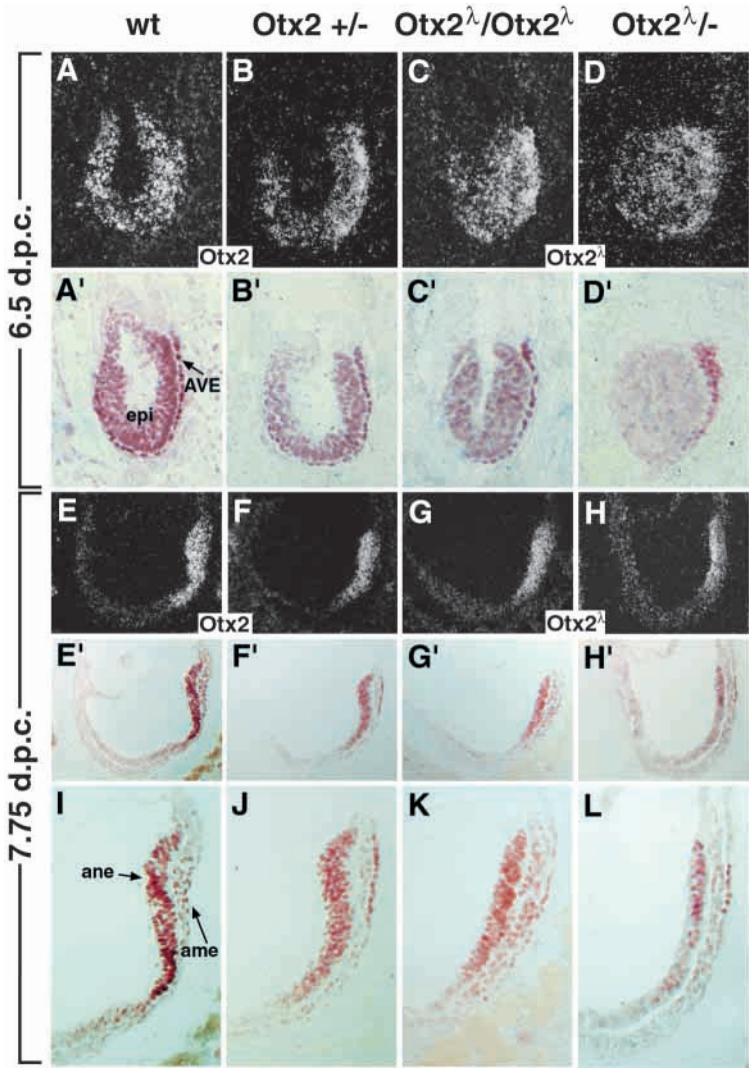

Fig. 3. Distribution of *Otx2*$^{\lambda}$ mRNA and protein during gastrulation. (A-L) Sagittal sections of 6.5 and 7.75 d.p.c. wild-type (A,A′,E,E′,I), *Otx2*$^{+/-}$ (B,B′,F,F′,J), *Otx2*$^{\lambda}$/*Otx2*$^{\lambda}$ (C,C′,G,G′,K) and *Otx2*$^{\lambda}$/– (D,D′,H,H′,L) embryos hybridised with an *Otx2*- (A,B,E,F) and an *Otx2*$^{\lambda}$ (C,D,G,H) -specific probe. There are no differences between *Otx2* (A,B,E,F) and *Otx2*$^{\lambda}$ (C,D,G,H) expression patterns. OTX2 protein levels are gradually reduced in the epiblast, anterior neuroectoderm and axial mesendoderm but not in the VE of *Otx2*$^{\lambda}$/*Otx2*$^{\lambda}$ (C',G',K) and *Otx2*$^{\lambda}$/– (D',H',L) mutants (when compared with wild-type (A',E',I) and *Otx2*$^{+/-}$ (B',F',J) embryos. ame, axial mesendoderm; ane, anterior neuroectoderm; AVE, anterior visceral endoderm; epi, epiblast. (I-L) Magnifications of embryos in (E′-H′).

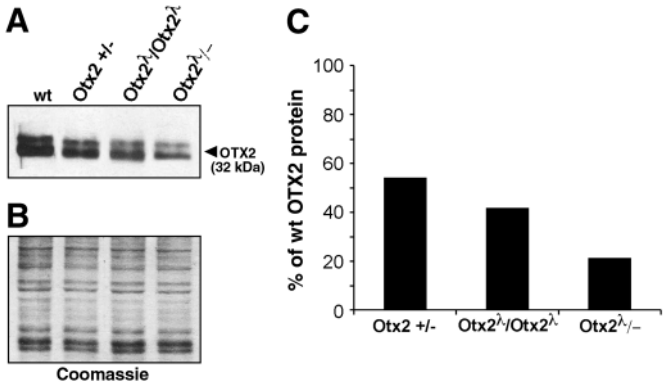

Fig. 4. OTX2 protein level in *Otx2*$^{\lambda}$ mutant embryos. (A) Western blot analysis of 7.5 d.p.c. wild-type, *Otx2*$^{+/-}$, *Otx2*$^{\lambda}$/*Otx2*$^{\lambda}$ and *Otx2*$^{\lambda}$/– embryos, showing that in *Otx2*$^{\lambda}$ mutants the OTX2 protein is remarkably reduced. (B) Coomassie Blue staining of the same gel in A. (C) Graphic representation of densitometric scanning indicating a reduction of ~60% of OTX2 protein in *Otx2*$^{\lambda}$/*Otx2*$^{\lambda}$ and *Otx2*$^{\lambda}$/– mutants when compared with wild-type and *Otx2*$^{+/-}$ embryos, respectively.

distribution of *Otx2*$^{\lambda}$ mRNA appeared unaffected in the epiblast and VE at 6.5 d.p.c. (compare Fig. 3A,B with 3C,D), as well as in ane and ame at 7.75 d.p.c. (compare Fig. 3E,F with 3G,H). Immunodetection of adjacent sections was performed with an anti-OTX2 polyclonal antibody (α-OTX2) (Mallamaci et al., 1996; Acampora et al., 1998b). The specificity of this antibody to OTX proteins has been previously assessed (Acampora et al., 1998b). At 6.5 d.p.c., in wild-type (Fig. 3A′) and *Otx2*$^{+/-}$ (Fig. 3B′) embryos, the OTX2 protein was detected with a similar strength in the epiblast and VE, even if in *Otx2*$^{+/-}$ embryos it appeared uniformly reduced.

At the same stage, in contrast with a robust expression of the *Otx2*$^{\lambda}$ mRNA, the OTX2$^{\lambda}$ protein levels became selectively reduced in the epiblast cells, while they remained high in the VE (Fig. 3C′,D′), an important internal control in these experiments.

At 7.75 d.p.c., the general scenario did not change. Indeed, while the *Otx2*$^{\lambda}$ mRNA distribution appeared to be normal (compare Fig. 3E,F with 3G,H), the OTX2$^{\lambda}$ protein diminished. In particular, the staining of *Otx2*$^{\lambda}$/*Otx2*$^{\lambda}$ embryos was similar to that of *Otx2*$^{+/-}$ and weaker than that of wild-type embryos (compare Fig. 3G′,K with 3F′,J and 3E′,I), while in *Otx2*$^{\lambda}$/– (Fig. 3H′,L) it appeared to be severely decreased. In all the 7.75 d.p.c. *Otx2*$^{\lambda}$/– embryos (n=6), the OTX2$^{\lambda}$-positive cells were localised in the rostralmost neuroectoderm and displayed heterogeneity in the strength of the signal (Fig. 3L).

Next, the OTX2$^{\lambda}$ protein level was assessed by performing western blot assays on independent pools of wild-type, *Otx2*$^{+/-}$, *Otx2*$^{\lambda}$/*Otx2*$^{\lambda}$ and *Otx2*$^{\lambda}$/– embryos at 7.5 d.p.c. (see also Materials and Methods). Very similar results were obtained in these experiments, indicating that the amounts of OTX2$^{\lambda}$ protein in *Otx2*$^{\lambda}$/*Otx2*$^{\lambda}$ and *Otx2*$^{\lambda}$/– embryos were, respectively, 40% and 20% of the one measured in wild-type embryos (Fig. 4A-C), and 90% and 40% of that detected in *Otx2*$^{+/-}$ embryos (Fig. 4A-C).

These findings, therefore, indicate that the λ insertion was sufficient to markedly affect the level of the OTX2$^{\lambda}$ protein in the epiblast and derived tissues but not in the VE.

Reduced ability of *Otx2*$^{\lambda}$ mRNA to form efficient polyribosome complexes

In order to determine the molecular events that were impaired in the post-transcriptional control of the *Otx2*$^{\lambda}$ mRNA, we studied whether the *Otx2*$^{\lambda}$ mRNA was efficiently transcribed, processed and translated in heterozygous *Otx2*$^{\lambda}$/*Otx2* embryos. *Otx2*$^{\lambda}$ and wild-type mRNAs were simultaneously detected by using the probe c (Fig. 1A and see also Materials and Methods). RNAse protection experiments were performed to detect total, cytoplasmic and nuclear transcripts that were quantified by phosphorimager scanning.

Compared with the wild-type *Otx2* mRNA, total, cytoplasmic and nuclear *Otx2*$^{\lambda}$ mRNA levels had decreased by approximately 20% (Fig. 5A), suggesting that this decrease cannot alone be sufficient to explain both OTX2$^{\lambda}$ protein decrease and phenotypic abnormalities. Moreover, as nuclear and cytoplasmic *Otx2*$^{\lambda}$ mRNAs underwent a similar reduction, nucleo-cytoplasmic export and processing should be unaffected. On this basis, the quantitative reduction should be ascribed to perturbation in transcription and/or stabilisation of the *Otx2*$^{\lambda}$ mRNA. In this context, however, actinomycin D experiments performed in the *Otx2*$^{\lambda}$/*Otx2* ES cell line did not reveal any difference in half life between the wild-type and the *Otx2*$^{\lambda}$ mRNAs ($t_{1/2}$=90 minutes) (data not shown). From these data, we suspect that the targeting vector may interfere with transcription of *Otx2* mRNA.

Next, we analysed the ability of *Otx2*$^{\lambda}$ and *Otx2* cytoplasmic mRNAs to form polyribosome complexes, in order to assess whether the translation of the *Otx2*$^{\lambda}$ mRNA was impaired. Cytoplasmic extracts from 10.5 d.p.c. heads were fractionated on sucrose gradients (see Materials and Methods). In a pilot experiment, in vitro synthesised *Otx2*$^{\lambda}$ RNA was added to a wild-type cytoplasmic extract to give a negative control. β-actin and wild-type *Otx2* were analysed in the same assay. According to the length of the β-actin (350 amino acid) and OTX2 (289 amino acid) proteins, ~50% of the β-actin and *Otx2* mRNAs was concentrated in the first two fractions, corresponding to the ones that contained polyribosome complexes with >10 and 8-10 ribosomes respectively, while ~70% of the in vitro synthesised *Otx2*$^{\lambda}$ RNA was concentrated in fractions that contained the 40S and 60S subunits (Fig. 5B).

The same experiment was performed on *Otx2*$^{\lambda}$/*Otx2* embryos at 7.75 d.p.c. and 10.5 d.p.c. (Fig. 5C,D). Interestingly, while β-actin and *Otx2* mRNAs were correctly distributed, only ~25% of the *Otx2*$^{\lambda}$ mRNA was detected in the first two fractions.

The percentage of *Otx2* and *Otx2*$^{\lambda}$ mRNAs detected in the third fraction was similar (Fig. 5C,D), while the percentage of *Otx2*$^{\lambda}$ mRNA in the second fraction was remarkably inferior. This suggests that the *Otx2*$^{\lambda}$ mRNA was affected in its ability to form the most efficient polyribosome complexes. Altogether, these data indicate that the reduced level of OTX2$^{\lambda}$ protein is largely due to an impairment of *Otx2*$^{\lambda}$ mRNA translation.

Proper onset and abnormal maintenance of forebrain and midbrain territory in *Otx2*$^{\lambda}$ mutants

In order to characterise the morphological defects of *Otx2*$^{\lambda}$ mutant embryos, the expression patterns of several diagnostic genes were analysed.

At 6.5 d.p.c., the expression of *Otx2*$^{\lambda}$, *cer-l*, *Lim1* and

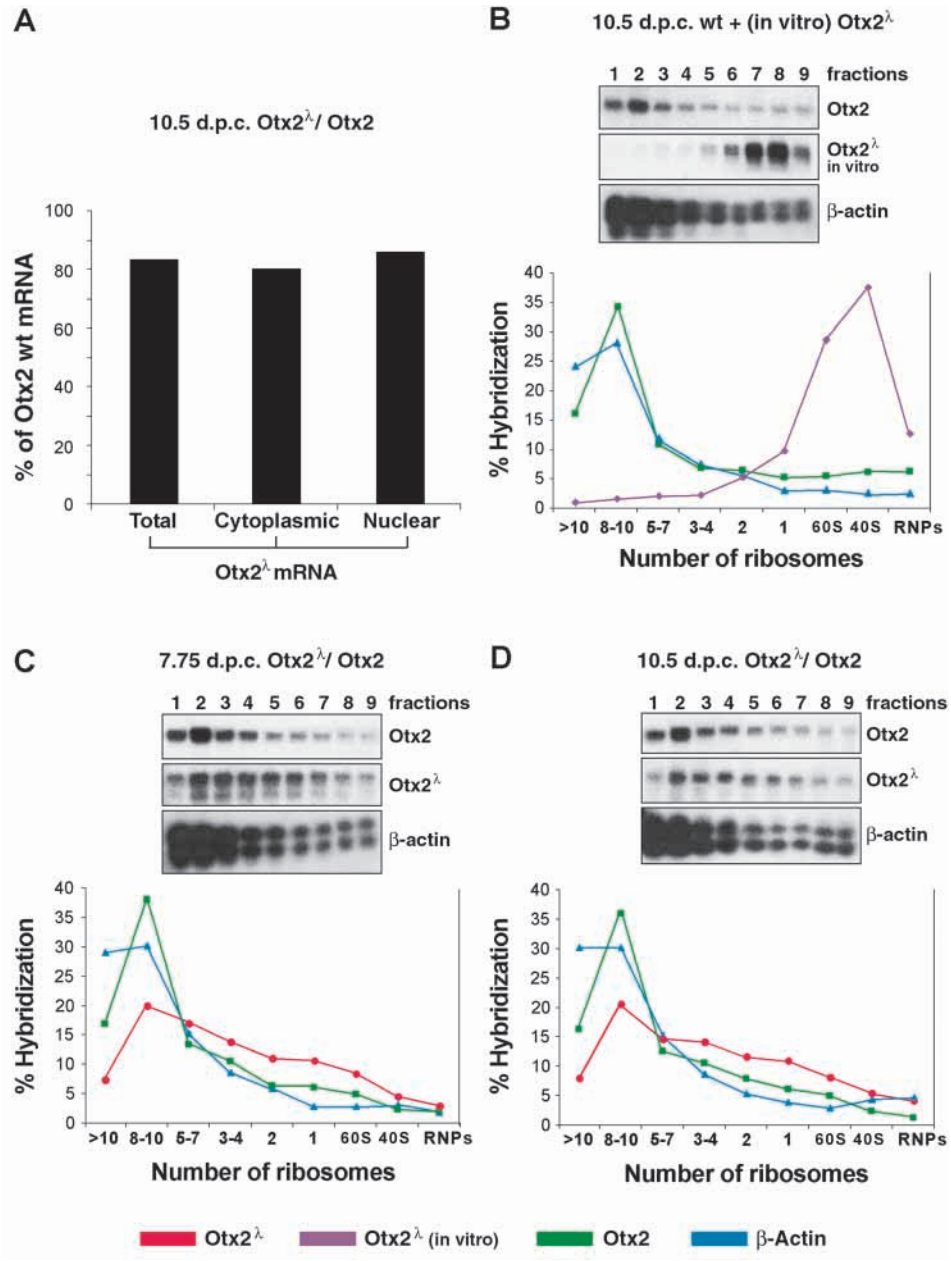

Fig. 5. Quantitative analysis and ribosome affinity profiles of *Otx2*$^{\lambda}$ mRNA. (A) Total, cytoplasmic and nuclear *Otx2*$^{\lambda}$ mRNA exhibits a reduction of ~20% when compared with the wild-type *Otx2* mRNA. The *Otx2*$^{\lambda}$ mRNA percentages are the mean of three independent experiments. (B) Ribosome affinity profiles of *Otx2*, β-actin mRNAs and in vitro synthesised *Otx2*$^{\lambda}$ RNA, showing the distribution of the untranslated *Otx2*$^{\lambda}$ RNA (see also Materials and Methods). (C,D) Ribosome affinity profiles comparing *Otx2*$^{\lambda}$, *Otx2* and β-actin mRNAs in *Otx2*$^{\lambda}$/*Otx2* embryos at 7.75 (C) and 10.5 d.p.c. (D) show that while more than 50% of the β-actin and *Otx2* mRNAs is detected in the first two fractions, only ~25% of the *Otx2*$^{\lambda}$ mRNA is concentrated in the same fractions. Note that mRNA profiles are not influenced by any quantitative variation of the mRNAs analysed.

goosecoid (*Gsc*) (not shown) revealed no abnormalities either in the AVE or the primitive streak of *Otx2*$^{\lambda}$/*Otx2*$^{\lambda}$ (data not shown) and *Otx2*$^{\lambda}$/– (Fig. 6B,D,F) embryos, thus indicating that none of the *Otx2*-dependent VE impairments were evident (Acampora et al., 1995; Acampora et al., 1998b; Matsuo et al., 1995; Ang et al., 1996; Rhinn et al., 1998).

The expression analysis of *Otx2*, *Otx2*$^{\lambda}$, *Gbx2*, *Six3*, *Chordin* (*Chd*) and *Lim1* genes was performed at 7.5 d.p.c. in *Otx2*$^{\lambda}$/*Otx2*$^{\lambda}$, *Otx2*$^{\lambda}$/– and wild-type embryos. In normal embryos, the anterior border of *Gbx2* was adjacent to the posterior one of *Otx2* (Fig. 6G,I), *Six3* was expressed in the rostralmost neuroectoderm fated to become telencephalon (Fig. 6K), and *Chd* and *Lim1* were transcribed in the node and ame (Fig. 6M,O). The expression pattern of these genes was highly perturbed or absent in *Otx2*$^{-/-}$ embryos (Acampora et al., 1995; Acampora et al., 1998b; Matsuo et al., 1995; Ang et al., 1996; Rhinn et al., 1998).

In all the *Otx2*$^{\lambda}$/*Otx2*$^{\lambda}$ (data not shown) and *Otx2*$^{\lambda}$/– (Fig. 6H,J,L,N,P) embryos, all these markers were correctly expressed and retained their spatial relationships. Therefore, despite the selective depletion of OTX2$^{\lambda}$ protein in the epiblast, ane and ame, the OTX2$^{\lambda}$ protein synthesised in the VE was sufficient to promote normal specification of early anterior pattern.

Morphological abnormalities of *Otx2*$^{\lambda}$/*Otx2*$^{\lambda}$ and *Otx2*$^{\lambda}$/– embryos became evident at 8.5-8.75 d.p.c., and were obvious at 10.5 d.p.c. Forebrain and midbrain regional identities along the rostral CNS were assessed at 8.5 d.p.c. and 10.5 d.p.c. by analysing the expression of *Otx2* (forebrain and midbrain territory (Figs 7A, 8A)), *Fgf8* and *Gbx2* (the isthmic primordium at the mid-hindbrain boundary (MHB) (Figs 7D,G, 8D,G)), *Wnt1* (the midbrain (Fig. 7J)) and *BF1* (the forebrain (Figs 7M, 8M)).

In abnormal *Otx2*$^{\lambda}$/*Otx2*$^{\lambda}$ embryos at 8.5 d.p.c., the expression of these markers was perturbed. *Otx2* was detected along an extended area, including the presumptive forebrain and midbrain territory but displaying two different levels of transcripts defined by two sharp borders of expression (black and red arrows in Fig. 7B). Interestingly, *Fgf8* and *Gbx2* (Fig. 7E,H) were moderately expanded and their new domains, fitted within the posterior area of lower expression of *Otx2*. *Wnt1* (Fig. 7K) and *BF1* (Fig. 7N), appeared to be less affected.

In *Otx2*$^{\lambda}$/– embryos, the expression patterns were more abnormal. The *Otx2* expression domain was smaller (Fig. 7C), and unable to antagonise anterior spread of *Fgf8* and *Gbx2* transcripts that were remarkably anteriorised within the *Otx2*

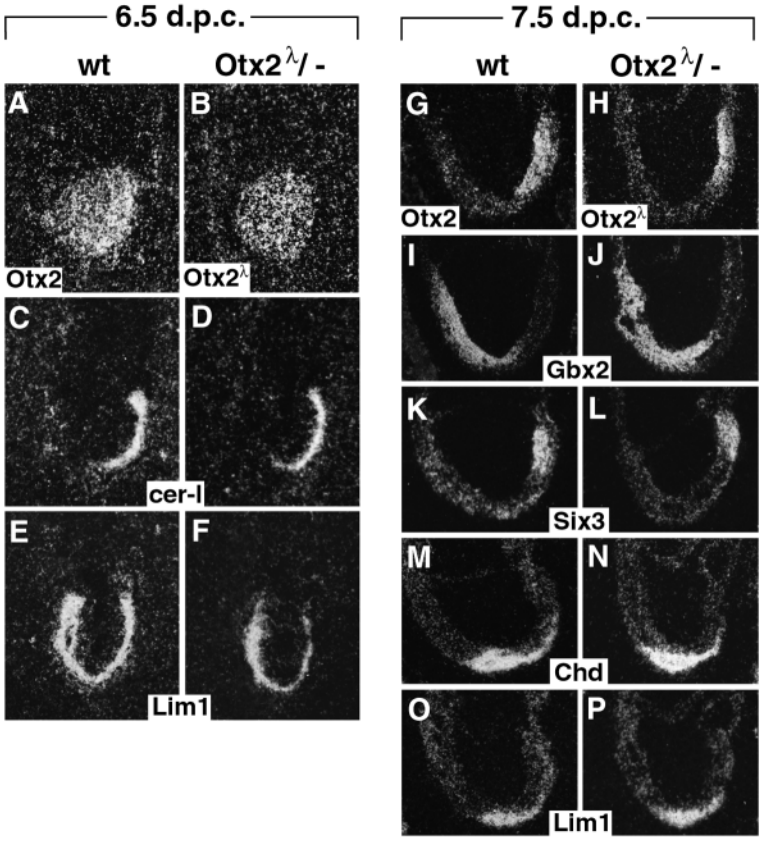

Fig. 6. Gastrulation and early patterning of rostral neuroectoderm are unaffected in *Otx2*$^{\lambda}$/– embryos. (A-F) Sagittal sections of 6.5 d.p.c. wild-type (A,C,E) and *Otx2*$^{\lambda}$/– (B,D,F) embryos hybridised with *Otx2* (A), *Otx2*$^{\lambda}$ (B), *cer-l* (C,D) and *Lim1* (E-F). (G-P) Sagittal sections of 7.5 d.p.c. wild-type (G,I,K,M,O) and *Otx2*$^{\lambda}$/– (H,J,L,N,P) embryos are hybridised with *Otx2* (G), *Otx2*$^{\lambda}$ (H), *Gbx2* (I,J), *Six3* (K,L) *Chd* (M,N) and *Lim1* (O,P).

expression domain (Fig. 7F,I). *Wnt1* was expressed in the rostralmost neuroectoderm (Fig. 7L) and *BF1* expression was not detected in the anterior neuroectoderm (Fig. 7O). At 10.5 d.p.c., in *Otx2*$^{\lambda}$/*Otx2*$^{\lambda}$, *Otx2*$^{\lambda}$ was expressed in a smaller domain (Fig. 8B); *Fgf8* (Fig. 8E) and *Gbx2* (Fig. 8H) were slightly expanded within the posterior domain of *Otx2* expression; and *BF1* was detected in a smaller domain of the presumptive telencephalon (Fig. 8K). In *Otx2*$^{\lambda}$/– embryos, *Otx2*$^{\lambda}$ (Fig. 8C) was transcribed along the rostralmost neuroectoderm; *Fgf8* (Fig. 8F) and *Gbx2* (Fig. 8I) transcripts were detected along an extended area largely overlapping the *Otx2*$^{\lambda}$ positive domain; and *BF1* (Fig. 8R) was never detected, thus indicating the lack of forebrain region.

These findings indicate that impairment of *Otx2* translational control in epiblast-derived cells (ane and ame) is reflected in severe abnormalities of rostral CNS.

A highly conserved sequence in the *Otx2*-3′ UTR of vertebrates

Our data indicated that the λ insertion interfered with translational control of *Otx2*$^{\lambda}$ mRNA but they did not help in identifying potential regulatory elements within the *Otx2*-3′ UTR.

For this purpose, a computer screening analysis for conserved sequences within the 3′ UTR was performed. For most 3′ UTRs, the sequence became available only recently (see Materials and Methods). Strikingly, from this analysis it appeared that a 140 bp long sequence element was fully conserved in all the *Otx2*-3′ UTRs of gnathostomes such as human, mouse, chicken, frog and zebrafish and a vestigial portion (26 bp long) was present in lamprey, an agnathan vertebrate (Fig. 9A-C).

No significant homology was detected in the *Otx2*-3′ UTRs of more primitive species such as protochordates (cephalochordates and tunicates), echinoderms (sea urchin) and insects (*Drosophila*) or in any other sequence (see also Materials and Methods). Interestingly, the 140 bp element was a unique feature of vertebrate *Otx2* genes, and among these it was fully conserved in gnathostomes that exhibited a similar plan of brain organisation. Indeed, in agnathes (lamprey), only a small portion of the element was conserved and noteworthy: even though the basic organisation of the rostral CNS was similar to gnathostomes, the topography and relative extent of different areas appeared remarkably different (Nieuwenhuys, 1998; Pombal and Puelles, 1999).

Hence, the λ insertion between the stop codon and the conserved element might have affected the stability and/or the formation of secondary structure(s) required for the binding of regulatory factor(s) or for the assembly of efficient polyribosome complexes. Therefore, sequence analysis has revealed a highly conserved element in the *Otx2*-3′ UTRs of gnathostome vertebrates having a common plan of brain organisation. We propose that this element may represent a positive regulator acquired during evolution and promoting or enhancing translation of *Otx2* mRNA in epiblast or neuronal progenitor cells. In this context, the vestigial conservation of the lamprey *Otx2*-3′ UTR may represent a transient and still evolutionary unstable condition.

DISCUSSION

Translational control in development

Spatial and temporal control of gene expression allows cells to acquire appropriate fates during morphogenesis. This control plays a crucial role in regulating the requirement of genetic determinants involved in inductive and differentiative processes, such as those defined by the interaction between organizer cells releasing instructing signals and responding target tissues. In particular, patterning of the anterior neuroectoderm in mouse is achieved by sequential steps involving initial activation of the anterior neural fate mediated by signal(s) emitted by the AVE, followed by a second phase required to stabilise, maintain and regionalise the anterior neuroectoderm (Beddington and Robertson, 1999; Stern, 2001).

This second phase is mediated by vertical signal(s) from the ame directed to the overlying neuroectoderm and planar signals from local organising centres such as the anterior neural ridge and the isthmic organizer (IsO) operating in the plane of the

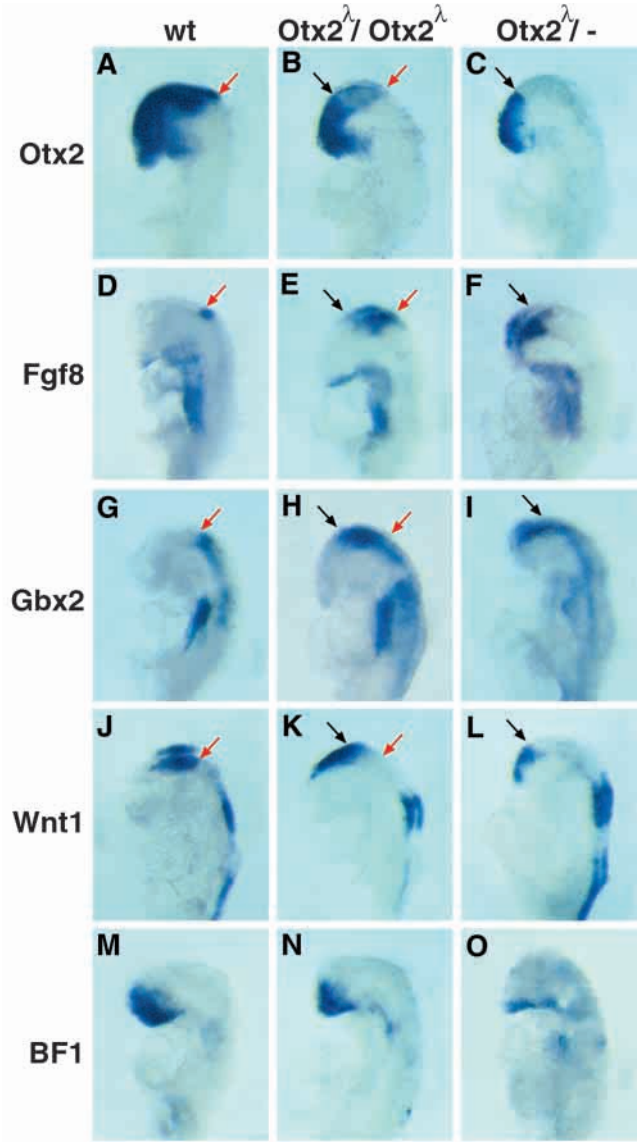

Fig. 7. Abnormal patterning of forebrain and midbrain territory in *Otx2*$^{\lambda}$/*Otx2*$^{\lambda}$ and *Otx2*$^{\lambda}$/– mutant embryos. (A-O) Whole-mount in situ hybridisation of 8.5 d.p.c. wild-type (A,D,G,J,M), *Otx2*$^{\lambda}$/*Otx2*$^{\lambda}$ (B,E,H,K,N) and *Otx2*$^{\lambda}$/– (C,F,I,L,O) embryos with probes for *Otx2* (A-C), *Fgf8* (D-F), *Gbx2* (G-I), *Wnt1* (J-L) and *BF1* (M-O).

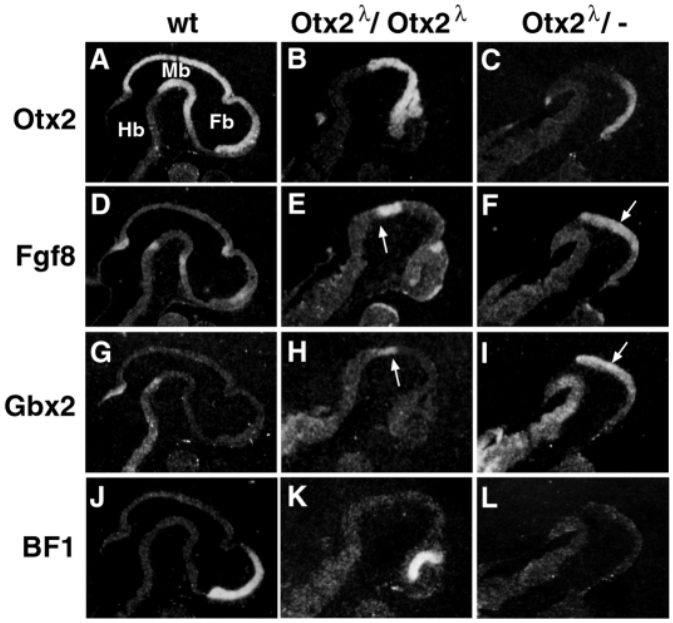

Fig. 8. Head abnormalities in *Otx2*$^{\lambda}$/*Otx2*$^{\lambda}$ and *Otx2*$^{\lambda}$/– embryos at 10.5 d.p.c. (A-L) Sagittal sections of 10.5 d.p.c. wild-type (A,D,G,J), *Otx2*$^{\lambda}$/*Otx2*$^{\lambda}$ (B,E,H,K) and *Otx2*$^{\lambda}$/– (C,F,I,L) embryos hybridised with probes for *Otx2* (A-C), *Fgf8* (D-F), *Gbx2* (G-I) and *BF1* (J-L). The arrows point to the corresponding position of the *Otx2* posterior border of expression. Fb, forebrain; Hb, hindbrain; Mb, midbrain.

neuroectoderm (Martinez et al., 1991; Crossley et al., 1996; Shimamura and Rubenstein, 1997; Beddington and Robertson, 1999; Stern, 2001; Wurst and Bally-Cuif, 2001).

A precise hierarchy of transcriptional events regulate the sequential activation of genes controlling the formation of body plan as well as the fate of different cell types. This final event is mediated by molecular interactions generating gradients of morphogenetic signals (De Robertis et al., 2000). Translational control plays a leading role in regulating fate decisions during cell differentiation and embryonic development (Curtis et al., 1995; Dubnau and Struhl, 1996; Gavis et al., 1996; Rivera-Pomar et al., 1996; Preiss and Hentze, 1999; Ostareck et al., 2001). In *Drosophila* oogenesis and early embryogenesis, translational regulation has been shown to be essential for the generation of protein gradients and determination of both the embryonic axis and cell fate (Curtis et al., 1995; Gavis et al., 1996). Interactions between 5′ and 3′ UTR sequences represent a constant and important molecular aspect of this control.

Nevertheless, to our knowledge no examples of such translational control have so far been provided during early decisions regarding specification and maintenance of early anterior patterning in mouse.

The analysis of a previous mouse mutant where *Otx2* is replaced with human *OTX1* has suggested differential post-transcriptional control of the *OTX1* mRNA between the VE and epiblast cells that is maintained during subsequent development of the rostral neuroectoderm. The lack of OTX proteins in epiblast and neuroectoderm is invariably reflected in the lack of forebrain and midbrain identity (Acampora et al., 1998b; Acampora and Simeone, 1999).

This led us to hypothesise that the *Otx2* replaced region might contain regulatory elements required for its post-transcriptional control (mRNA processing and/or translation). Alternatively, as in *OTX1* mutants the *Otx2* locus was heavily engineered, abnormal non physiological molecular events affecting RNA stability, processing, transport or translation may be responsible for the lack of human OTX1 protein.

To settle this important issue, we have generated a mouse model carrying a 300 bp long insertion of exogenous DNA of the λ phage within the *Otx2*-3′ UTR, with the aim of perturbing *Otx2* post-transcriptional control in the epiblast and derived tissues. Our findings have indicated that translation of *Otx2*$^{\lambda}$ mRNA is markedly impaired in the epiblast and neuroectoderm of mutant embryos but not in the VE.

Transcription was only slightly reduced and processing

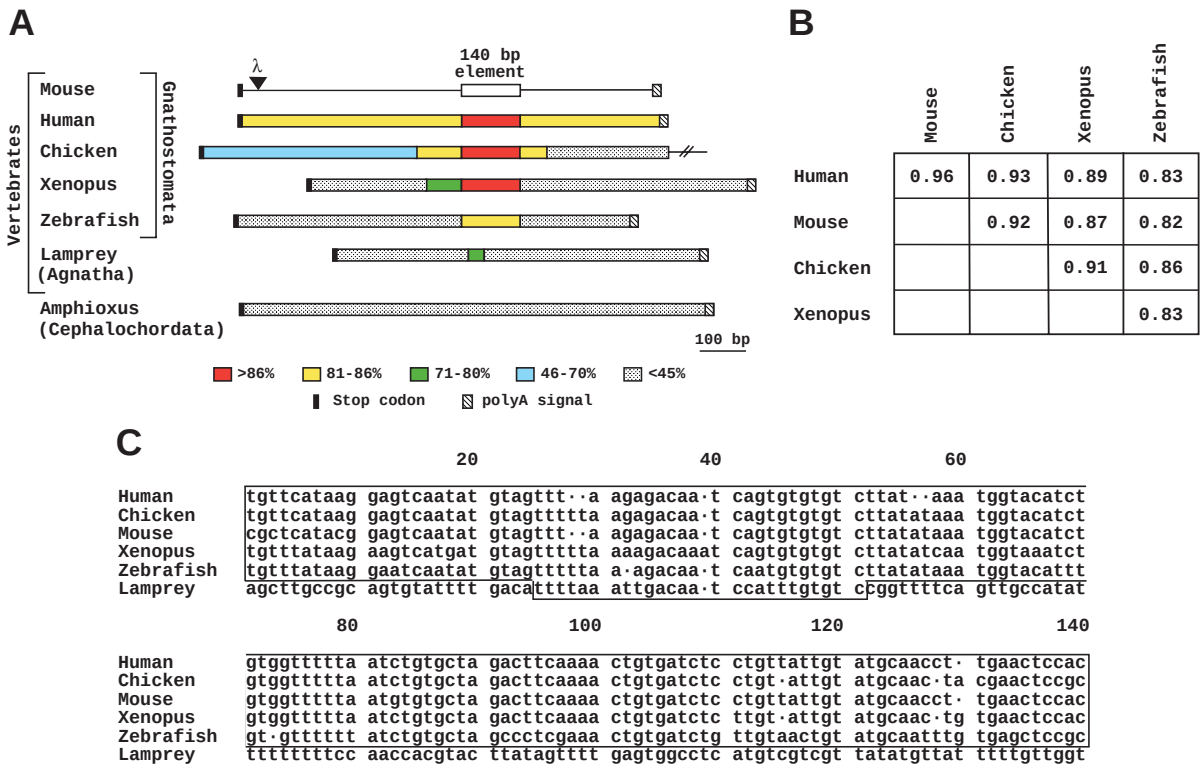

Fig. 9. Vertebrate *Otx2* genes contain a conserved element within the 3′ UTR. (A) Schematic alignment between the mouse and the human, chicken, *Xenopus*, zebrafish, lamprey and *Amphioxus Otx2* 3′ UTRs, showing the conserved 140 bp element. Percentages of homology between corresponding regions are reported with different colours. In lamprey, only 26 bp of the element are conserved. (B) Percentages of identity of the 140 bp element among the reported gnathostomata. (C) DNA sequence alignment of the conserved element, also including the 26 bp conserved sequence of the lamprey.

and nucleo/cytoplasmic export of $Otx2^{\lambda}$ mRNA appeared unaffected. The relevance of this impairment in translational control was highlighted by head abnormalities detected in $Otx2^{\lambda}/Otx2^{\lambda}$ and $Otx2^{\lambda}/-$ embryos.

Otx2 is one of the genetic determinants that plays a significant role in patterning the rostral neuroectoderm (reviewed by Simeone, 1998; Simeone, 2000; Acampora and Simeone, 1999; Stern 2001; Wurst and Bally-Cuif, 2001) and, indeed, from late gastrula/early somite stage onward, it performs this role by both positioning the IsO at the MHB and conferring appropriate competence to neural tissue responding to inductive signals from the IsO (Simeone, 2000; Wurst and Bally-Cuif, 2001; J. P. M.-B. and A. S., unpublished).

This *Otx2*-dependent function is highly sensitive to variations in protein level. Indeed, reduction below a critical threshold or ectopic gain of OTX2 protein correspond to reduction or increase in the size of forebrain and midbrain territory, respectively (Simeone, 2000; Wurst and Bally-Cuif, 2001). $Otx1^{-/-}; Otx2^{+/-}$ double mutants display transformation of midbrain and posterior diencephalon in an expanded metencephalon (Acampora et al., 1997); in $hOtx1^{2}/hOtx1^{2}$ embryos, the entire forebrain and midbrain are replaced with the metencephalon (Acampora et al., 1998b), while, by contrast, mice expressing *Otx2* under *En1* transcriptional control move the MHB posteriorly and increase the extent of the posterior midbrain (Broccoli et al., 1999).

We have shown that $Otx2^{\lambda}$ mutants (Fig. 2C) exhibit two additional hypomorphic phenotypes: $Otx2^{\lambda}/Otx2^{\lambda}$ mutants were similar to $Otx1^{-/-}; Otx2^{+/-}$ double mutants or revealed a moderate anterior repositioning of the MHB and additional abnormalities affecting the size and the shape of forebrain, as well as the closure of neural tube (Figs 2B and 8); 90% of $Otx2^{\lambda}/-$ mutants was almost headless (Fig. 2D). Even a relatively small reduction of OTX2 protein below a critical threshold corresponding to a normal single copy was phenotypically translated in head abnormalities. Indeed, compared with $Otx2^{+/-}$ embryos that are viable and fertile, $Otx2^{\lambda}/Otx2^{\lambda}$ showed a 10% reduction in the OTX2 protein and 65% of them revealed head abnormalities.

Therefore, these results provide evidence that *Otx2* may have developed a regulatory mechanism that allows its efficient translation in epiblast and derived tissues. This positive control has permitted the availability of a critical amount of OTX2 protein sufficient and necessary to maintain and/or stabilise early forebrain and midbrain regional identities.

Impaired translation of *Otx2* mRNA in epiblast but not in VE

The aim of this work has been to demonstrate the existence and molecular nature of the *Otx2* post-transcriptional control acting in epiblast and neuronal progenitors, in order to finely regulate the appropriate amount of OTX2 protein. We have demonstrated that a sequence perturbation in the 3′ UTR affects the ability of the $Otx2^{\lambda}$ mRNA to form efficient polyribosome complexes. Indeed, the $Otx2^{\lambda}$ mRNA is able to bind ribosomes but exhibits an intrinsic difficulty to be

complexed with the expected number of ribosomes. Indeed, when compared with the sharp and abundant (~40%) peak of the wild-type *Otx2* mRNA, only ~20% of the *Otx2*$^{\lambda}$ mRNA is distributed in the same fraction containing the most efficient number of ribosomes and ~80% is spread in those fractions containing fewer ribosomes or single ribosome subunits. Moreover, the *Otx2*$^{\lambda}$ mRNA is not sequestered into translationally silent ribonucleic particles and is not concentrated in the fraction corresponding to the 40S.

This profile suggests that the progressive recruitment of ribosomes is affected. In this context, formation of the small ribosomal subunit-initiation factor complex or scanning of the 5′ UTR by the complex before the identification of the AUG initiator codon might be affected. The presence of secondary structures in the 5′ UTR sequence might interfere or delay ribosome scanning (Curtis et al., 1995; Preiss and Hentze, 1999).

In this context, the *Otx2*-5′ UTR sequence may potentially give rise to stable stem-loop structures (data not shown). Nevertheless, as the only structural abnormality in the *Otx2*$^{\lambda}$ transcription unit affects the 3′ UTR, an eventual impairment in ribosomal scanning should imply that the 3′ and 5′ UTRs interact with each other to relieve the structural block. This being the case, our findings are more compatible with a reduced efficiency of the 3′ UTR in interacting with the 5′ UTR. This may explain why efficient polyribosome complexes are assembled but in a reduced number. Additional impairment caused by the λ DNA insertion may involve the correct formation of RNA secondary structure(s) that interact with factor(s) necessary to control polyadenylation or cellular localisation of the mRNA (Curtis et al., 1995; Preiss and Hentze, 1999). These factors may operate as translational repressors or enhancers. Nevertheless, while further experiments are required to address which translational control mechanism is affected, our data have provided direct evidence that VE and epiblast cells possess differential translational control properties with respect to the *Otx2*$^{\lambda}$ mRNA. This phenomenon is particularly intriguing because it is revealed only when a mutant *Otx2* mRNA is analysed. Indeed, the wild-type *Otx2* mRNA is translated in all the cells in which it is transcribed, thus indicating that the translational control highlighted in the *Otx2*$^{\lambda}$ mutants is normally bypassed. This implies that VE cells should possess a translational control machinery that is able to translate *Otx2* mRNA independently from its sequence complexity, whereas epiblast cells should be provided with a different translational control machinery competent to translate only the wild-type *Otx2* mRNA.

This observation is also strengthened by previous mouse models replacing *Otx2* with *OTX1* cDNA, or *lacZ* or *Drosophila otd* cDNA (Acampora et al., 1995; Acampora et al., 1998b; D. A. and A. S., unpublished). However, it cannot be excluded that translational control of *Otx2* mRNA might be affected also in the VE. Nevertheless VE-restricted property mediated by OTX2 appeared unaffected. When compared with epiblast cells, this might be due to a more efficient accumulation of OTX2 protein or to a higher rate of *Otx2* gene transcription.

Translational control of *Otx2* and vertebrate brain evolution

Compared with other genes translationally regulated to perform important decisions during embryonic development and/or cell differentiation (Curtis et al., 1995; Dubnau and Struhl, 1996; Rivera-Pomar et al., 1996; Preiss and Hentze, 1999; Ostareck at al., 2001), the *Otx2* translational control should be considered from a different perspective: it might represent an acquired gain of function that has eluded epiblast-restricted negative translational control. As a consequence, the forebrain and midbrain maintenance property has been conferred to neuronal precursor cells.

The direct correlation between efficient translation of *Otx2* mRNA in neuronal progenitor cells and maintenance of forebrain and midbrain territory may have important evolutionary implications. Stabilisation of forebrain and midbrain territory, and appropriate OTX2 protein level may be a direct consequence of efficient translational control acquired during evolution. Should this be the case, it is conceivable that regionalisation of forebrain and midbrain territory, and translational control of *Otx2* mRNA appear contemporary and are inseparable. Therefore, this control should have been established or improved when an elaborated brain with obvious regionalisation appears during evolution. Indeed, the architectural components of the vertebrate brain (telencephalon, diencephalon and mesencephalon) are much less clear in protochordates, including cephalochordates and tunicates (Kuhlenbeck, 1973; Nieuwenhuys, 1998).

On this basis, it may be argued that the original and more primitive function of *Otx2* was probably restricted to VE-like cells, in order to instruct proper gastrulation and to contribute to activation of specification of the anterior neuroectoderm but not to its maintenance. Moreover, as suggested by *Otx2*-null embryos, OTX2 protein was required in VE cells also to mediate *Otx2* transcriptional activation in epiblast cells. (Acampora et al., 1995). Therefore, it is conceivable that the invariable transcription of *Otx2* in the anterior neuroectoderm of protochordates and chordates is the consequence of its primary function in the primitive endoderm (Wada et al., 1996; Williams and Holland, 1996; Williams and Holland, 1998; Reichert and Simeone, 1999). Epiblast restricted translation of *Otx2* mRNA might represent a secondary regulatory event that is coincident to and responsible for a deep modification of fate and morphogenesis of anterior neuroectoderm. This event, together with other important molecular modifications involving gene duplication and diversification, recruitment of new genetic functions into pre-existing developmental pathways and the establishment of new developmental pathways, may have greatly contributed to define and refine the basic genetic program underlying the evolution of the vertebrate brain.

Accordingly, modification of *Otx2* translational control might have contributed to the evolution of the mammalian brain; for example, by increasing the extent of neuroectodermal territory recruited to form the brain. This event might involve an improvement of proliferative activity of early neuronal progenitors (Acampora et al., 1998a; Acampora et al., 1999) and/or the positioning of the MHB (Acampora et al., 1997; Acampora et al., 1998b; Suda et al., 1997). Interestingly, computer analysis has indicated that the *Otx2*-3′ UTR of all gnathostome vertebrates analysed retains a highly conserved 140 bp long element (> 80% of identity) whereas in lamprey, the length of the conserved element is reduced to 26 bp. No significant homology is detected in the *Otx2*-3′ UTR from protochordates, echinoderms and insects or with any other sequence.

This structural conservation is evident only in those species possessing a regionalised brain (vertebrate brain), and our in vivo data do not exclude that the *Otx2* positive translational control may be functionally related to the conserved element. Accordingly, it is tempting to speculate that it may represent the vertebrate positive regulatory element that, by mediating epiblast-restricted translational control of *Otx2* mRNA, has contributed to instruct brain morphogenesis. Forthcoming mouse models will experimentally address this crucial issue.

We thank Andrew Lumsden for critical reading of the manuscript and helpful discussions. We also thank J. Zeto Belo for the *chordin* probe, and A. Secondulfo and S. Borgarelli for manuscript preparation. This work was supported by the MRC (Grant Number: G9900955), the Italian Association for Cancer Research (AIRC), the EU BIOTECH programme (Number: BIO4-CT98-0309), the MURST-CNR Biotechnology Programme Legge 95/95, the MURST-CNR Programme Legge 488/92 (cluster 02) and the Fondation Bettencourt Schueller.

REFERENCES

Acampora, D., Mazan, S., Lallemand, Y., Avantaggiato, V., Maury, M., Simeone, A. and Brûlet, P. (1995). Forebrain and midbrain regions are deleted in *Otx2*$^{-/-}$ mutants due to a defective anterior neuroectoderm specification during gastrulation. *Development* **121**, 3279-3290.

Acampora, D., Mazan, S., Avantaggiato, V., Barone, P., Tuorto, F., Lallemand, Y., Brûlet, P. and Simeone, A. (1996). Epilepsy and brain abnormalities in mice lacking *Otx1* gene. *Nat. Genet.* **14**, 218-222.

Acampora, D., Avantaggiato, V., Tuorto, F. and Simeone, A. (1997). Genetic control of brain morphogenesis through *Otx* gene dosage requirement. *Development* **124**, 3639-3650.

Acampora, D., Avantaggiato, V., Tuorto, F., Barone, P., Reichert, H., Finkelstein, R. and Simeone, A. (1998a). Murine *Otx1* and *Drosophila otd* genes share conserved genetic functions required in invertebrate and vertebrate brain development. *Development* **125**, 1691-1702.

Acampora, D., Avantaggiato, V., Tuorto, F., Briata, P., Corte, G. and Simeone, A. (1998b). Visceral endoderm-restricted translation of *Otx1* mediates recovering of *Otx2* requirements for specification of anterior neural plate and proper gastrulation. *Development* **125**, 5091-5104.

Acampora, D., Avantaggiato, V., Tuorto, F., Barone, P., Perera, M., Choo, D., Wu, D., Corte, G. and Simeone, A. (1999). Differential transcriptional control as the major molecular event in generating *Otx1*$^{-/-}$ and *Otx2*$^{-/-}$ divergent phenotypes. *Development* **126**, 1417-1426.

Acampora, D. and Simeone, A. (1999). Understanding the roles of *Otx1* and *Otx2* in controlling brain morphogenesis. *Trends Neurosci.* **22**, 116-122.

Ang, S.-L., Jin, O., Rhinn, M., Daigle, N., Stevenson, L. and Rossant, J. (1996). Targeted mouse *Otx2* mutation leads to severe defects in gastrulation and formation of axial mesoderm and to deletion of rostral brain. *Development* **122**, 243-252.

Beddington, R. S. and Robertson, E. J. (1999). Axis development and early asymmetry in mammals. *Cell* **96**, 195-209.

Biltz, I. L. and Cho, K. W. (1995). Anterior neuroectoderm is progressively induced during gastrulation: the role of the *Xenopus* homebox gene *orthodenticle*. *Development* **121**, 993-1004.

Broccoli, V., Boncinelli, E. and Wurst, W. (1999). The caudal limit of *Otx2* expression positions the isthmic organizer. *Nature* **401**, 164-168.

Crossley, P. H., Martinez, S. and Martin, G. R. (1996). Midbrain development induced by FGF8 in the chick embryo. *Nature* **380**, 66-68.

Curtis, D., Lehmann, R. and Zamore, P. D. (1995). Translational regulation in development. *Cell* **81**, 171-178.

De Robertis, E. M. and Sasai, Y. (1996). A common plan for dorsoventral patterning in the Bilateria. *Nature* **380**, 37-40.

De Robertis, E. M., Larraìn, J., Oelgeschläger, M. and Wessely, O. (2000). The stablishment of Spemman's organizer and patterning of the vertebrate embryo. *Nat. Rev. Genet.* **1**, 171-181.

Dubnau, J. and Struhl, G. (1996). RNA recognition and translational regulation by a homeodomain protein. *Nature* **379**, 694-699.

Finkelstein, R., Smouse, D., Capaci, T. M., Spradling, A. C. and Perrimon, N. (1990). The *orthodenticle* gene encodes a novel homeodomain protein involved in the development of the *Drosophila* nervous system and ocellar visual structures. *Genes Dev.* **4**, 1516-1527.

Gavis, E. R., Lunsford, L., Bergsten, S. E. and Lehmann, R. (1996). A conserved 90 nucleotide element mediates translational repression of nanos RNA. *Development* **122**, 2791-2800.

Hogan, B., Beddington, R., Costantini, F. and Lacy, E. (1994). In *Manipulating the Mouse Embryo. A Laboratory Manual*. 2nd edn. New York: Cold Spring Harbor Laboratory Press.

Holland, P. W. H. (1999). The future of evolutionary developmental biology. *Nature* **402 Suppl.**, C41-C44.

Kuhlenbeck, H. (1973). *The Central Nervous System of Vertebrates.* Basel: Karger.

Li, Y., Allende, M. L., Finkelstein, R. and Weinberg, E. S. (1994). Expression of two zebrafish *orthodenticle*-related genes in the embryonic brain. *Mech. Dev.* **48**, 229-244

Loreni, F. and Amaldi, F. (1992). Translational regulation of ribosomal protein synthesis in *Xenopus* cultured cells: mRNA relocation between polysomes and RNA during nutritional shifts. *Eur. J. Biochem.* **205**, 1027-1032.

Mallamaci, A., Di Blas, E., Briata, P., Boncinelli, E. and Corte, G. (1996). OTX2 homeoprotein in the developing central nervous system and migratory cells of the olfactory area. *Mech. Dev.* **58**, 165-178.

Martinez, S., Wassef, M. and Alvarado-Mallart, R.-M. (1991). Induction of a mesencephalic phenotype in the 2 day-old chick prosencephalon is preceded by the early expression of the homeobox gene *en*. *Neuron* **6**, 971-981.

Matsuo, I., Kuratani, S., Kimura, C., Takeda, N. and Aizawa, S. (1995). Mouse *Otx2* functions in the formation and patterning of rostral head. *Genes Dev.* **9**, 2646-2658.

Nieuwenhuys, R. (1998). Morphogenesis and general structure: In *The Central Nervous System Of Vertebrates*. Vol. 1 (ed. R. Nieuwenhuys, H. J. ten Donkelaar and C. Nicholson), pp. 159-228. Berlin: Springer Verlag.

Ostareck, D. H., Ostareck-Lederer, A., Shatsky, I. N. and Hentze, M. W. (2001). Lipoxygenase mRNA silencing in erythroid differentiation: the 3′ UTR regulatory complex controls 60S ribosomal subunit joining. *Cell* **104**, 281-290.

Pombal, M. A. and Puelles, L. (1999). Prosomeric map of the lamprey forebrain based on calretinin immunocytochemistry, Nissl stain, and ancillary markers. *J. Comp. Neurobiol.* **414**, 391-422.

Preiss, T. and Hentze, M. (1999). From factors to mechanisms: translation and translational control in eukaryotes. *Curr. Opin. Gen Dev.* **9**, 515-521.

Reichert, H. and Simeone, A. (1999). Conserved usage of gap and homeotic genes in patterning the CNS. *Curr. Opin. Neurobiol.* **9**, 589-595.

Rhinn, M., Dierich, A., Shawlot, W., Behringer, R. R., Le Meur, M. and Ang, S.-L. (1998). Sequential roles for *Otx2* in visceral endoderm and neuroectoderm for forebrain and midbrain induction and specification. *Development* **125**, 845-856.

Rivera-Pomar, R., Niessing, D., Schmidt-Ott, U., Gehring, W.J. and Jäckle, H. (1996). RNA binding and translational suppression by *bicoid*. *Nature* **379**, 746-749.

Rubenstein, J. L. R., Shimamura, K., Martinez, S. and Puelles, L. (1998). Regionalization of the prosencephalic neural plate. *Annu. Rev. Neurosci.* **21**, 445-477.

Sakamoto, N., Akasaka, K., Mitsunaga-Nakatsubo, K., Takata, K., Nishitani, T. and Shimada, H. (1997). Two isoforms of *orthodenticle*-related proteins (HpOtx) bind to the enhancer element of *sea urchin* arylsulfatase gene. *Dev. Biol.* **181**, 284-295.

Shimamura, K. and Rubenstein, J. L. R. (1997). Inductive interactions direct early regionalization of the mouse forebrain. *Development* **124,** 2709-2718.

Simeone, A., Acampora, D., Gulisano, M., Stornaiuolo, A. and Boncinelli, E. (1992). Nested expression domains of four homeobox genes in developing rostral brain. *Nature* **358**, 687-690.

Simeone, A., Acampora, D., Mallamaci, A., Stornaiuolo, A., D'Apice, M. R., Nigro, V. and Boncinelli, E. (1993). A vertebrate gene related to *orthodenticle* contains a homeodomain of the *bicoid* class and demarcates anterior neuroectoderm in the gastrulating mouse embryo. *EMBO J.* **12**, 2735-2747.

Simeone, A. (1998). *Otx1* and *Otx2* in the development and evolution of the mammalian brain. *EMBO J.* **17**, 6970-6978.

Simeone, A. (1999). Detection of mRNA in tissue sections with radiolabelled riboprobes. In *In Situ Hybridization. A Practical Approach.* 2nd edn (ed. D. G. Wilkinson), pp 69-86. Oxford: IRL, Oxford University Press.

Simeone, A. (2000). Positioning the isthmic organizer where *Otx2* and *Gbx2* meet. *Trends Genet.* **16**, 237-240.

Stern, C. (2001). Initial patterning of the central nervous system: how many organizers? *Nat. Rev. Neurosci.* **2**, 92-98.

Suda, Y., Matsuo, I. and Aizawa, S. (1997). Cooperation between *Otx1* and *Otx2* genes in developmental patterning of rostral brain. *Mech. Dev.* **69**, 125-141.

Tam, P. P. L. and Behringer, R. R. (1997). Mouse gastrulation: the formation of a mammalian body plan. *Mech. Dev.* **68**, 3-25.

Ueki, T., **Kuratani, S., Hirano, S. and Aizawa, S.** (1998). *Otx* cognates in a lamprey, *Lampetra japonica*. *Dev. Genes Evol.* **208**, 223-228.

Wada, S., **Katsuyama, Y., Sato, Y., Itoh, C. and Saiga, H.** (1996). *Hroth* an *orthodenticle*-related homeobox gene of the ascidian, *Halocynthia roretzi*: its expression and putative roles in the axis formation during embryogenesis. *Mech. Dev.*, **60**, 59-71.

Williams, N. A. and Holland, P. W. H. (1996). Old head on young shoulders. *Nature* **383**, 490.

Williams, N. A. and Holland, P. W. (1998). Gene and domain duplication in the chordate *Otx* gene family: insights from *amphioxus Otx*. *Mol. Biol. Evol.* **15**, 600-607.

Wurst, W. and Bally-Cuif, L. (2001). Neural plate patterning: upstream and downstream of the isthmic organizer. *Nat. Rev. Neurosci.* **2,** 99-108.